Journal of Chromatography A, 1230 (2012) 77–92

Contents lists available at SciVerse ScienceDirect

Journal of Chromatography A

journal homepage: www.elsevier.com/locate/chroma

Bypass chromatography – design and analysis of an improved strategy for operating batch chromatography processes

Jani Siitonen[a], Tuomo Sainio[a,*], Arvind Rajendran[b]

[a] Lappeenranta University of Technology, Skinnarilankatu 34, FIN-53850 Lappeenranta, Finland
[b] Nanyang Technological University, School of Chemical and Biomedical Engineering, 62 Nanyang Drive, Singapore 637459, Singapore

ARTICLE INFO

Article history:
Received 27 September 2011
Received in revised form 22 January 2012
Accepted 25 January 2012
Available online 31 January 2012

Keywords:
Batch chromatography
Bypass
Reduced purity
Equilibrium theory
Process design

ABSTRACT

The possibility to improve the performance of batch chromatographic separations by using so-called bypass method is analyzed for the first time. In bypass chromatography, only a part of the feed is introduced into the column and purified to purity larger than the desired value. The resulting fractions are then blended with fresh feed to match the given purity constraints. A general approach is presented for designing bypass batch chromatography. Analytical design equations, based on equilibrium theory of chromatography, are presented for the case of binary systems with linear or competitive Langmuir adsorption isotherms under ideal conditions. The approach allows direct calculation of optimal loading and amount of bypass so that arbitrary purity requirements are satisfied without waste streams. It is shown that the bypass strategy enhances productivity of batch chromatography without an increase in the eluent consumption. In the case of a Langmuir isotherm, maximum productivity and minimum eluent consumption are always obtained when the less retained component is collected from the column at 100% purity. In contrast, the optimal purity of the second fraction from the column is typically less than 100% and depends on the purity constraint of the more retained component. In the case of linear isotherms, operation with touching bands is preferred.

1. Introduction

Preparative chromatographic separations are often designed with the aim of nearly complete separation of the feed mixture [1]. This is justified in applications within the pharmaceutical and fine chemical industry where very high product purities are demanded. However, there exist several practical applications where products with much lower purity are required, for example in the production of sweeteners [2] and agrochemicals [3]. Moreover, combining chromatography with complementary separation process, such as crystallization, provides the possibility to enhance the process performance [4,5]. In these operations it is customary to operate the chromatography unit under reduced purity constraints, while the final polishing step, *i.e.* increase the purity, is performed by the crystallization step.

The design of chromatographic processes with reduced purity constraints has recently received increased attention. Equilibrium theory based design methods have been derived for simulated moving bed chromatography in the case of linear [6] and Langmuir [7] isotherms, and for steady state recycling chromatography in the case of Langmuir isotherm [8–10]. In addition, there exist few approaches to optimize the operation conditions of batch chromatography when only one of the components of a binary mixture is considered as target [11,12].

When products with reduced purity are required, different operation strategies can be applied. Traditionally, the entire feed solution is processed in the column and the operating parameters are selected such that target purity constraints are fulfilled. In this work a second alternative is introduced, *i.e.* to overpurify only a part of the feed in the column and blend the resulting fractions with fresh feed to match the target purities. The former strategy will henceforth be called as "conventional chromatography" and the latter as "bypass chromatography".

The bypass mode has been used successfully, for instance, in the simulated moving bed (SMB) separation of fructose–glucose mixture to produce high-fructose corn syrup [2]. The key attraction of bypass chromatography comes from the fact that the implementation requires virtually no additional equipment and requires no modification in the existing chromatographic system. While there are examples of industrial applications, the theory of such bypass strategies has not been properly investigated and hence there is lack of explicit methods for analysis and optimal design of such

* Corresponding author. Tel.: +358 403578683; fax: +358 5 6212199.
E-mail address: tuomo.sainio@lut.fi (T. Sainio).

0021-9673/$ – see front matter © 2012 Elsevier B.V. All rights reserved.
doi:10.1016/j.chroma.2012.01.071

process concept. Moreover, systematic comparison of conventional and bypass operation modes has not been presented in the literature.

The objective of the present work is to investigate the possibility to enhance the performance of batch chromatography by employing the bypass strategy. For this purpose, local equilibrium theory is used to derive a method to choose the optimal operating parameters that lead to given purities in the bypass process. The approach is limited to ideal conditions and to circumstances where concentration profiles of consecutive injections are not allowed to overlap. Analytic design equations are provided for binary systems that follow Langmuir or linear adsorption isotherm model. The design method is then used to compare the performance of conventional and bypass batch processes. It is shown that by applying bypass strategy it is possible to enhance productivity of batch chromatography without an increase in the eluent consumption, provided that the purity constraints are less than 100%. Finally, a short discussion is given on the applicability of the equilibrium design approach for columns with finite efficiency.

2. Theoretical background

2.1. Equilibrium theory of chromatography

The equilibrium theory of chromatography is a powerful technique that has been used to design both single- [1,8,11] and multi-column [6,7] processes. Within the frame of the equilibrium theory, the mass transfer resistance and the dispersive effects are neglected. Under these conditions, the mass balance for an individual component i is given by

$$\frac{\partial}{\partial t}(c_i + \phi q_i) + u\frac{\partial c_i}{\partial x} = 0 \quad (i = 1, 2) \tag{1}$$

where c_i and q_i are the mobile and the stationary phase concentrations of solute i, $\phi = (1-\varepsilon)/\varepsilon$ is the phase ratio, with ε being the total void fraction of the bed, u is the interstitial velocity, t is time, and x is axial space coordinate.

In order to solve Eq. (1), the dependence between the stationary phase loading and the mobile phase concentration, *i.e.* the adsorption isotherm, is needed. In this work, the following two isotherm models are discussed: linear isotherm

$$q_i = H_i c_i \quad (i = 1, 2) \tag{2}$$

and competitive Langmuir isotherm

$$q_i = \frac{H_i c_i}{1 + K_1 c_1 + K_2 c_2} \quad (i = 1, 2) \tag{3}$$

where H_i and K_i are the Henry constant and the Langmuir parameter of solute i, respectively. In the following discussion it is assumed that component 1 is the less absorbed one, which means that $H_2 > H_1$.

The model forms a system of two partial differential equations and can be solved analytically both for linear and competitive Langmuir isotherm systems. For a comprehensive discussion of the theory, the interested reader is referred to more detailed works [13–17].

2.2. Design specifications

In the following discussion, it is assumed that a binary mixture is separated into two product fractions so that no waste or recycle streams are generated. The less adsorbed component 1 is the target constituent in the product fraction A and the more retained component 2 in the product fraction B. The desired purities of the fractions are kept as design constraints:

$$p_1^{\mathrm{A}} = \frac{m_1^{\mathrm{A}}}{m_1^{\mathrm{A}} + m_2^{\mathrm{A}}} \tag{4}$$

$$p_2^{\mathrm{B}} = \frac{m_2^{\mathrm{B}}}{m_1^{\mathrm{B}} + m_2^{\mathrm{B}}} \tag{5}$$

where m_i^j is the amount of component $i = (1, 2)$ in the product fraction $j = (\mathrm{A}, \mathrm{B})$.

As an alternative to the use of purities as a design constraint, the yields of the components in the target fractions can be given. Because no waste stream is allowed, the purity and yield requirements are interchangeable [4]

$$Y_1 = \frac{m_1^{\mathrm{A}}}{m_1^{\mathrm{F}}} = \frac{p_1^{\mathrm{A}}}{p_1^{\mathrm{F}}}\frac{p_1^{\mathrm{F}} + p_2^{\mathrm{B}} - 1}{p_1^{\mathrm{A}} + p_2^{\mathrm{B}} - 1} \tag{6}$$

$$Y_2 = \frac{m_2^{\mathrm{B}}}{m_2^{\mathrm{F}}} = \frac{p_2^{\mathrm{B}}}{1 - p_1^{\mathrm{F}}}\frac{p_1^{\mathrm{A}} - p_1^{\mathrm{F}}}{p_1^{\mathrm{A}} + p_2^{\mathrm{B}} - 1} \tag{7}$$

where p_1^{F} is defined as the purity of component 1 in feed: $p_1^{\mathrm{F}} = c_1^{\mathrm{F}}/(c_1^{\mathrm{F}} + c_2^{\mathrm{F}})$. This means that by specifying any two of the four constraints, the remaining two are also fixed.

3. Principle of bypass operation

The basic principle of the bypass operation strategy of batch chromatography is illustrated in Fig. 1. During each chromatographic cycle, *i.e.* injection, a constant amount of fresh feed, V^{PF}, is introduced to the process. As opposed to the conventional operation of batch chromatography, only a certain portion of this stream is fed into the column and separated into two fractions. The rest of the fresh feed bypasses the column, and is blended with the two fractions from the column in a certain proportion to match the overall target purity constraints, p_1^{A} and p_2^{B}.

The amount of feed injected into the chromatographic column, V_{inj}, is chosen such that the purities of both intermediate fractions, p_1^{CA} and p_2^{CB}, satisfy the following requirements: $p_1^{\mathrm{CA}} \geq p_1^{\mathrm{A}}$ and $p_2^{\mathrm{CB}} \geq p_2^{\mathrm{B}}$. In other words, V_{inj} must always be lower than the volume that can be processed in conventional batch process such that desired target purities are satisfied.

Examples of typical concentration profiles at column outlet are shown in Fig. 2 for three different cases. The chromatographic cycle starts at time t_{R1} when the first component begins to elute. Between t_{R1} and the cut time t_{cut}, the chromatographic fraction CA, which contains an excess of the less retained component, *i.e.* 1, is collected. After t_{cut}, the column effluent is directed to fraction CB to collect the more retained component, *i.e.* 2, until the chromatogram is eluted completely at time t_{E2}. Finally, both chromatographic fractions CA and CB are blended with fresh feed to match the actual purity constraints, p_1^{A} and p_2^{B}. The fractions bypassed are quantified by

$$\beta^{\mathrm{A}} = \frac{\text{volume of feed bypassed to fraction A}}{\text{total volume of fresh feed processed}} \tag{8}$$

$$\beta^{\mathrm{B}} = \frac{\text{volume of feed bypassed to fraction B}}{\text{total volume of fresh feed processed}} \tag{9}$$

Note that $\beta^{\mathrm{A}} + \beta^{\mathrm{B}} + V_{\mathrm{inj}}/V^{\mathrm{PF}} = 1$.

Fig. 3 shows a demonstrative example of the influence of p_1^{CA} and p_2^{CB} on different operating and performance parameters of bypass chromatography. Total fresh feed volume, V^{PF}, injection volume, V_{inj}, productivity, PR and specific eluent consumption EC are expressed as ratio, R_j, between these quantities in bypass and batch

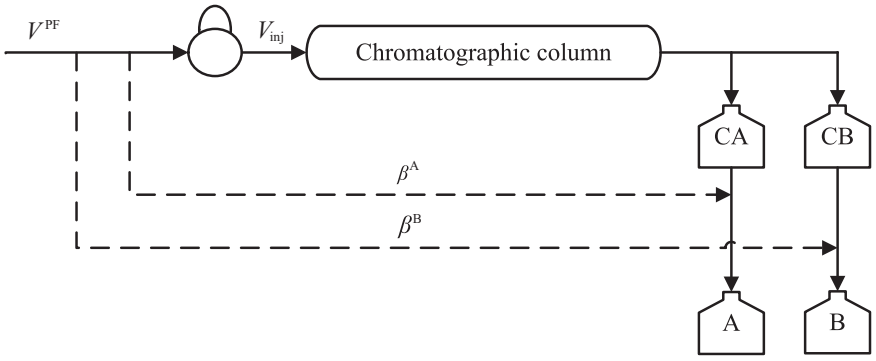

Fig. 1. Schematic representation of a bypass process. V^{PF}, total volume of fresh feed to the process; V_{inj}, injection volume into the column; β^A bypass ratio to product fraction A; β^B bypass ratio to product fraction B; CA, first column fraction; CB second column fraction; A, product fraction A; B, product fraction B.

processes. As seen in Fig. 3a, it is not possible to increase the total amount of fresh feed that can be processed in conventional batch chromatography by applying bypass. However, the purer the components are collected from the column, the larger portion of fresh feed can be bypassed (Fig. 3b) and the smaller the injection volume is (Fig. 3a). This means that the increase in performance achieved by using bypass (Fig. 3c) results from the decrease in the injection volume (and thus the cycle time) and not from the increase in the total amount of fresh feed that is introduced to the process during a chromatographic cycle.

At this point, it should be emphasized that bypass operation can be implemented without any additional equipment or columns. The only additional tasks beyond the conventional operation are splitting of the feed stream into column and bypass fractions and,

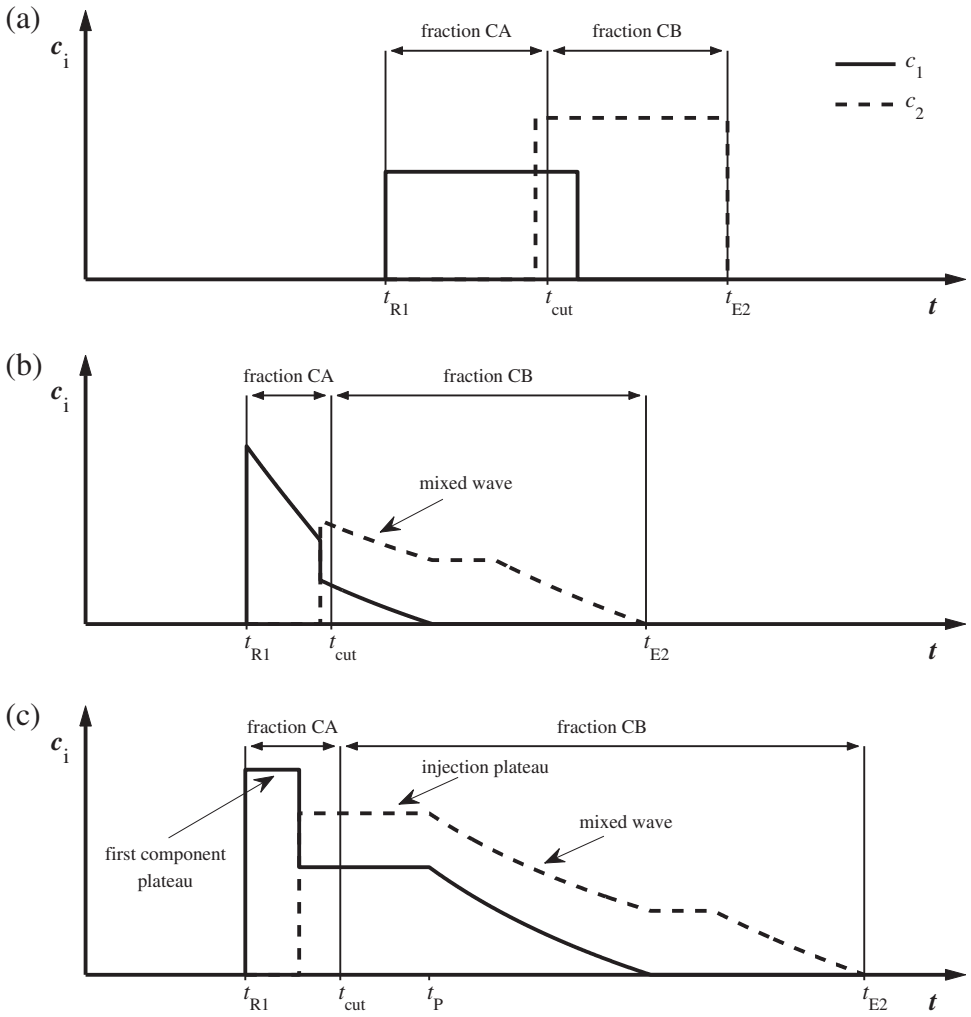

Fig. 2. Individual elution profiles of a rectangular injection pulse for an arbitrary system and fraction collection in bypass batch chromatography. (a) Linear isotherm. (b) Langmuir isotherm, small injection. (c) Langmuir isotherm, large injection.

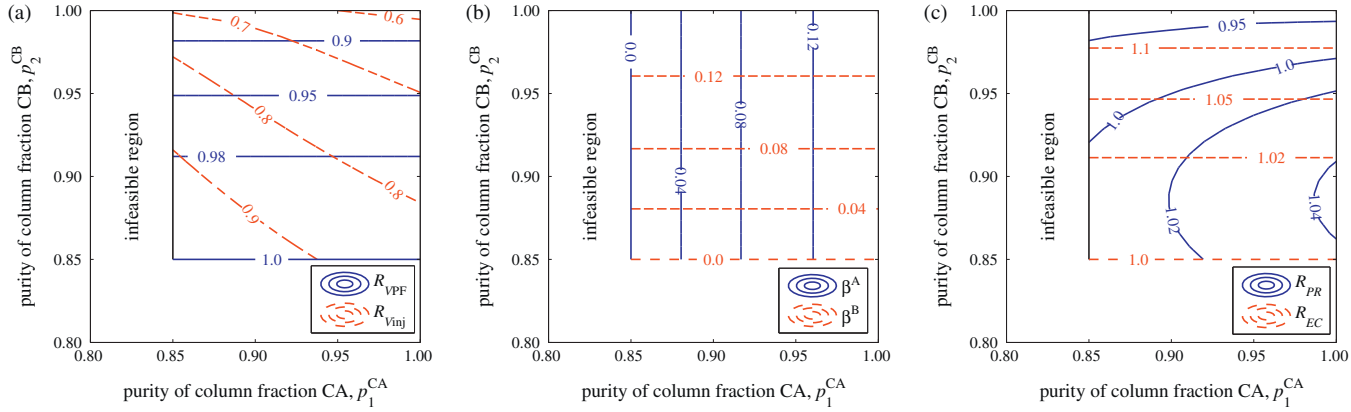

Fig. 3. Effect of purities of the column fractions on the operating and performance parameters of bypass process relative to that of conventional batch chromatography in the separation of Tröger's base enantiomers. Isotherm parameters are given in Section 7. Feed concentrations: $c_1^F = c_2^F = 6$ g/L. Purity constraints: $p_1^A = p_2^B = 0.85$.

after the separation, blending of the two column fractions with bypass stream. This makes the strategy attractive for practical purposes.

4. Design of bypass chromatography

In this section, a simple design method for single column bypass chromatography is derived. The task is to find the bypass ratios β^A and β^B, the volumes V^{PF} and V_{inj}, and the cut time t_{cut} that lead to given product purities, p_1^A and p_2^B, when the purities of the column fractions, p_1^{CA} and p_2^{CB}, are specified. The latter can be chosen freely as long as $p_1^{CA} \geq p_1^A$ and $p_2^{CB} \geq p_2^B$. Optimization of p_1^{CA} and p_2^{CB} is discussed later in Section 5.

4.1. Calculation of the bypass ratios β^A and β^B

A fundamental characteristic of bypass operation is that the bypass ratios, β^A and β^B, can be calculated directly from the purities of the column fractions without knowing V^{PF} and V_{inj}. This is observed by considering the individual mass balances of the components. The yield of component 1 can be written with the mass of the first column fraction, *i.e.* fraction CA, as follows

$$Y_1 = \frac{\beta^A m_1^{PF} + m_1^{CA}}{m_1^{PF}} = \beta^A + \frac{m_1^{CA}}{c_1^F V^{PF}} \tag{10a}$$

and with the mass of the second column fraction, CB, as follows

$$Y_1 = \frac{\beta^A m_1^{PF} + [(1-\beta^A-\beta^B)m_1^{PF} - m_1^{CB}]}{m_1^{PF}} = 1 - \beta^B - \frac{m_1^{CB}}{c_1^F V^{PF}} \tag{10b}$$

For the second component, the corresponding equations are

$$Y_2 = \frac{\beta^B m_2^{PF} + [(1-\beta^A-\beta^B)m_2^{PF} - m_2^{CA}]}{m_2^{PF}} = 1 - \beta^A - \frac{m_2^{CA}}{c_2^F V^{PF}} \tag{11a}$$

$$Y_2 = \frac{\beta^B m_2^{PF} + m_2^{CB}}{m_2^{PF}} = \beta^B + \frac{m_2^{CB}}{c_2^F V^{PF}} \tag{11b}$$

The bypass ratio β^A is obtained by eliminating V^{PF} from Eqs. (10a) and (11a)

$$\beta^A = Y_1 - \frac{p_1^{CA}(1-p_1^F)(Y_1+Y_2-1)}{p_1^{CA}-p_1^F} \tag{12}$$

and the bypass ratio β^B by eliminating V^{PF} from Eqs. (10b) and (11b)

$$\beta^B = Y_2 - \frac{p_2^{CB}p_1^F(Y_1+Y_2-1)}{p_2^{CB}-(1-p_1^F)} \tag{13}$$

It should be emphasized that the above equations are obtained by considering only the mass balances. Further they are functions of the feed composition and the operating requirements, *i.e.* purity and yield, only. This means that they are independent of the isotherm type and, unlike the other results represented in this work, they are also valid under non-ideal conditions.

It is also worth noting that β^A and β^B increase when p_1^{CA} and p_2^{CB} increase, respectively. This is because the purer the column fractions are collected the more fresh feed can be blended into them to fulfill the purity constraints, p_1^A and p_2^B. The upper limits for the bypass ratios are $\beta_{max}^A = 1 - Y_2$ and $\beta_{max}^B = 1 - Y_1$. They are reached when p_1^{CA} and p_2^{CB} equal 100%.

4.2. Calculation of V^{PF}, V_{inj} and t_{cut}

Once the bypass ratios β^A and β^B are solved, the next task is to find V^{PF}, V_{inj} and t_{cut} that lead to given purities. Complete sets of design equations are provided for linear isotherm in Table 1 and for Langmuir isotherm in Table 2.

It is commonly known that for Langmuir and linear isotherms the shape of the rear part of the chromatogram is independent of the injection volume. It is only shifted in time by the duration of the injection, Δt_{inj} [8,16]. Based on this observation, the cut time relative to the end of the injection, $\tau_{cut} = t_{cut} - \Delta t_{inj}$, is selected such that the purity constraint of the column fraction CB is fulfilled. This is done by integrating the rear part of the chromatogram and searching for the lower integration limit that satisfies Eq. (14)

$$p_2^{CB} = \frac{\int_{\tau_{cut}}^{\tau_{E2}} c_2 d\tau}{\int_{\tau_{cut}}^{\tau_{E2}} (c_1+c_2) d\tau} \tag{14}$$

In the case of linear isotherm the cut point is always located on the injection plateau as shown in Fig. 2a, and is given by Eq. (1.1). For Langmuir isotherm there exist two options. If p_2^{CB} is high, the fractionation point is located on the mixed wave (Fig. 2b and Eq. (2.7)). In contrast, for sufficiently low p_2^{CB} values, the cut point lies on the injection plateau (Fig. 2c and Eq. (2.12)). The limit for these two cases is obtained by integrating the rear part of the chro-

Table 1
Design equations of bypass batch chromatography for linear isotherm. V_{col} is column volume.

$\tau_{cut} = \frac{p_2^{CB}(1+\phi H_1)c_1^F - (1-p_2^{CB})(1+\phi H_2)c_2^F}{p_2^{CB}c_1^F - (1-p_2^{CB})c_2^F} t_0$	(1.1)
$V^{PF} = \frac{(1-\varepsilon)(H_2-H_1)p_2^B c_1^F}{[p_2^B c_1^F - (1-p_2^B)c_2^F]Y_2} V_{col}$	(1.2)

Table 2
Design equations of bypass batch chromatography for Langmuir isotherm. V_{col} is column volume. λ is an auxiliary parameter. m_i^{rear} is mass of component i that elutes from column after the end of the injection plateau.

Slopes of characteristics and corresponding ω-parameters at feed state

$$\xi_+^F = \frac{\alpha - 1 + \alpha K_1 c_1^F - K_2 c_2^F + \sqrt{(\alpha - 1 + \alpha K_1 c_1^F - K_2 c_2^F)^2 + 4\alpha K_1 K_2 c_1^F c_2^F}}{2\alpha K_1 c_2^F} \quad (2.1)$$

$$\xi_-^F = \frac{\alpha - 1 + \alpha K_1 c_1^F - K_2 c_2^F - \sqrt{(\alpha - 1 + \alpha K_1 c_1^F - K_2 c_2^F)^2 + 4\alpha K_1 K_2 c_1^F c_2^F}}{2\alpha K_1 c_2^F} \quad (2.2)$$

$$\omega_1^F = \frac{H_1(\alpha K_1 \xi_-^F + K_2)}{K_1 \xi_-^F + K_2} \quad (2.3)$$

$$\omega_2^F = \frac{H_1(\alpha K_1 \xi_+^F + K_2)}{K_1 \xi_+^F + K_2} \quad (2.4)$$

Purity of the second fraction when the cut point is located at the end of the injection plateau

$$p_{2,\text{limitA}}^{CB} = \left[1 + \left(\frac{p_1^F}{1 - p_1^F}\right)^2 \frac{1}{\alpha \xi_+^F}\right]^{-1} \quad (2.5)$$

The cut point is located on the mixed wave, $p_2^{CB} > p_{2,\text{limitA}}^{CB}$

$$\lambda = \sqrt{\frac{1 - p_2^{CB}}{p_2^{CB}} \frac{1}{\alpha \xi_+^F}} \quad (2.6)$$

$$\tau_{cut} = t_0 + \frac{\phi \omega_2^F}{H_1 H_2} \left(\frac{H_1 - H_2 \lambda}{1 - \lambda}\right)^2 t_0 \quad (2.7)$$

$$V^{PF} = \frac{(1 - \varepsilon)(H_2 - H_1)(H_2 - \omega_2^F)}{K_2 H_2 c_2^F (Y_2 - \beta^B)} \left(\frac{1}{1 - \lambda}\right)^2 V_{col} \quad (2.8)$$

The cut point is located on the injection plateau, $p_2^{CB} \le p_{2,\text{limitA}}^{CB}$

$$\tau_P = t_0 + \frac{\phi (\omega_1^F)^2 \omega_2^F}{H_1 H_2} t_0 \quad (2.9)$$

$$m_1^{rear} = \frac{(1 - \varepsilon)(\omega_2^F - H_1)(H_1 - \omega_1^F)^2}{K_1 H_1 (H_2 - H_1)} V_{col} \quad (2.10)$$

$$m_2^{rear} = \frac{(1 - \varepsilon)(H_2 - \omega_2^F)(H_2 - \omega_1^F)^2}{K_2 H_2 (H_2 - H_1)} V_{col} \quad (2.11)$$

$$\tau_{cut} = \tau_P - \frac{m_2^{rear} - [p_2^{CB}/(1 - p_2^{CB})] m_1^{rear}}{[p_2^{CB}/(1 - p_2^{CB})] c_1^F - c_2^F} \frac{1}{Q} \quad (2.12)$$

$$V^{PF} = \frac{(\tau_P - \tau_{cut}) c_2^F Q + m_2^{rear}}{c_2^F (Y_2 - \beta^B)} \quad (2.13)$$

matogram from the end of the injection plateau τ_P to the end of the elution profile of the second component τ_{E2}

$$p_{2,\text{limitA}}^{CB} = \frac{\int_{\tau_P}^{\tau_{E2}} c_2 d\tau}{\int_{\tau_P}^{\tau_{E2}} (c_1 + c_2) d\tau} \quad (15)$$

Once the cut time τ_{cut} is obtained, also the amount of the column fraction B is known. The volume of fresh feed is solved from the mass balance of the component 2. The resulting expression for V^{PF} is given by

$$V^{PF} = \frac{Q \int_{\tau_{cut}}^{\tau_{E2}} c_2 d\tau}{c_2^F (Y_2 - \beta^B)} \quad (16)$$

where Q is flow rate. It is interesting to note that β^B and V^{PF} obtained from Eqs. (13) and (16) are independent of p_1^{CA} and V_{inj}. This means that specification of p_2^{CB} together with the overall purity constraints, p_1^A and p_2^B, determines how much fresh feed can be introduced to the whole process during a chromatographic cycle. This is a very important characteristic of bypass operation mode.

The final step of the design procedure is to calculate the portion of the fresh feed that is injected to the column. It is obtained from the global mass balance around the feed node

$$V_{inj} = \Delta t_{inj} Q = (1 - \beta^A - \beta^B) V^{PF} \quad (17)$$

4.3. Robustness of bypass operation

The process robustness, *i.e.* the sensitivity of the process against different disturbances, is an important issue related to all chromatographic separations. For example, even minor variations in fresh feed concentrations and flow rate affect the product quality when fraction collection is based on predetermined cut times. In bypass operation, this problem can be partly eliminated by determining the composition of the column fractions before blending them with the fresh feed. The amount of bypass can thus be adjusted to fulfill the purity constraints. This makes the bypass strategy more robust compared to conventional operation of single column batch chromatography. Moreover, if robustness is a major concern and the target purities are relatively high, V_{inj} can be decreased below its optimal value (see next section) to achieve clear baseline separation. This gives some safety margin for the cut time but naturally decreases the productivity to some extent.

5. Optimization of operating parameters of bypass chromatography

As usual in designing separation processes, it is important to optimize the operating parameters so that maximum process performance is achieved. In this case, these are the purities of the column fractions, p_1^{CA} and p_2^{CB}. Because the linear and the Langmuir isotherm systems have differences with respect to the optimal operating parameters, these two cases are treated separately: first the linear case in Section 5.1 and then the Langmuir case in Section 5.2.

In the following discussion, the process performance is evaluated in terms of productivity and specific eluent consumption. The productivity is defined as the amount of feed per the cycle time

$$PR = \frac{m_{tot}^A + m_{tot}^B}{\Delta t_{cycle}} = \frac{c_{tot}^F V^{PF}}{\Delta t_{cycle}} \quad (18)$$

where $c_{tot}^F = c_1^F + c_2^F$ is the total feed concentration. The specific eluent consumption is given by the ratio between the amount of eluent used in a chromatographic cycle, V_{eluent}, and the amount of feed

$$EC = \frac{V_{eluent}}{m_{tot}^A + m_{tot}^B} = \frac{(\Delta t_{cycle} - \Delta t_{inj}) Q}{c_{tot}^F V^{PF}} \quad (19)$$

When calculating the cycle time, it is assumed that the process is operated with "stacked injections" so that the chromatograms of consecutive injections do not overlap but there is no gap between them either. In this case, the cycle time is

$$\Delta t_{cycle} = t_{E2} - t_{R1} \quad (20)$$

It is worth noting that, in the case of reduced purity constraints, it is also possible to operate batch chromatography such that the consecutive injections do overlap. As shown in Appendix A, this kind of operation does not affect the process performance, and hence the conclusions of this optimization study for linear isotherm systems. As to Langmuir isotherm systems, this aspect was not investigated here because there are no analytical equations available to calculate the elution profiles of overlapping cycles.

Finally, it should be noted again that this work is limited to binary separations without a waste stream. For this reason, the productivities and the specific eluent consumptions of the individual components are proportional to the values obtained by Eqs. (18) and (19).

5.1. Optimization of operating parameters for linear isotherm systems

In the case of linear isotherm systems, the mixed zone of the chromatogram consists only of the feed plateau. For this reason, V^{PF} is always independent of both p_1^{CA} and p_2^{CB} as seen in Eq. (1.2). In fact, it is possible to process exactly the same amount of fresh feed per cycle by using bypass and conventional operation modes. This amount depends only on the isotherm parameters, feed composition and the purity constraints.

Because V^{PF} is independent of the purities of the column fractions, the optimization procedure for linear isotherm system under ideal conditions is very straightforward. To maximize the productivity of bypass operation, the cycle time must be minimized. In practice, this means that the process is operated with touching bands, and the purities of both the column fractions are 100%. This is understood by considering that generation of mixed fraction in the column always increases cycle time, and thus decreases productivity.

As to the specific eluent consumption, it is independent of the bypass ratios. This is because in the case of linear isotherm the injection width does not affect t_{R1} while the derivative t_{E2} with respect to Δt_{inj} is always equal to unity. The derivative $\partial\Delta t_{cycle}/\partial\Delta t_{inj}$ is thus also unity which yields

$$\frac{\partial EC}{\partial \Delta t_{inj}} = \frac{Q}{c_{tot}^{F} V^{PF}} \left(\frac{\partial \Delta t_{cycle}}{\partial \Delta t_{inj}} - 1 \right) = 0 \tag{21}$$

5.2. Optimization of operating parameters for Langmuir isotherm systems

5.2.1. Optimization of p_1^{CA}

In the case of Langmuir isotherm systems, V^{PF} depends on p_2^{CB} only, while it is independent of p_1^{CA} and V_{inj} as mentioned in Section 4.2. For this reason, p_1^{CA} affects the productivity and the specific eluent consumption through the injection width and the cycle time only. Based on these observations, it will be shown shortly that the optimal p_1^{CA} is independent of p_2^{CB}. Subsequently, optimization of p_2^{CB} for a certain p_1^{CA} will be discussed.

When p_2^{CB}, and thus also V^{PF}, is constant, the injection width decreases with increasing p_1^{CA}. This is observed by substituting β^A from Eq. (12) into Eq. (17) and differentiating the resulting equation with respect to p_1^{CA}

$$\left.\frac{\partial \Delta t_{inj}}{\partial p_1^{CA}}\right|_{p_2^{CB}} = -\frac{V^{PF}}{Q} \frac{p_1^{F}(1-p_1^{F})(Y_1+Y_2-1)}{(p_1^{CA}-p_1^{F})^2} < 0 \tag{22}$$

In addition, it has recently been shown that the derivative of Δt_{cycle} with respect to Δt_{inj} is always at least unity [17]

$$\frac{\partial \Delta t_{cycle}}{\partial \Delta t_{inj}} = \frac{\partial(\tau_{E2} + \Delta t_{inj} - t_{R1})}{\partial \Delta t_{inj}} = 1 - \frac{\partial t_{R1}}{\partial \Delta t_{inj}} \geq 1 \tag{23}$$

The equality sign refers to large injections where the first component plateau is not eroded during elution and the first shock propagates with constant velocity. For small injections, the first plateau erodes completely and the height of the shock decreases. In this case, the velocity of the shock decreases and t_{R1} increases with decreasing injection width.

By using Eqs. (22) and (23) together with the definition of productivity, Eq. (18), it is observed that the cycle time always decreases, and thus the productivity always increases, with increasing p_1^{CA}, *i.e.*

$$\left.\frac{\partial PR}{\partial p_1^{CA}}\right|_{p_2^{CB}} = -\frac{c_{tot}^{F} V^{PF} (\partial \Delta t_{cycle}/\partial \Delta t_{inj})(\partial \Delta t_{inj}/\partial p_1^{CA})}{(\Delta t_{cycle})^2} > 0 \tag{24}$$

This means that the maximum productivity is always obtained when p_1^{CA} is as high as possible, *i.e.* $p_1^{CA} = 100\%$.

For the evaluation of specific eluent consumption Eq. (19) is differentiated with respect to Δt_{inj}. Again, for large injections the first component plateau prevails and *EC* is independent of the injection width. In the case of small injections, an increase in *EC* is expected because $\partial\Delta t_{cycle}/\partial\Delta t_{inj}$ is greater than unity

$$\frac{\partial EC}{\partial \Delta t_{inj}} = \frac{Q}{c_{tot}^{F} V^{PF}} \left(\frac{\partial \Delta t_{cycle}}{\partial \Delta t_{inj}} - 1 \right) \geq 0 \tag{25}$$

By applying the chain rule to Eqs. (22) and (25) it is observed that *EC* decreases monotonically or remains constant with increasing p_1^{CA}

$$\left.\frac{\partial EC}{\partial p_1^{CA}}\right|_{p_2^{CB}} \leq 0 \tag{26}$$

As seen from Eqs. (24) and (26), both maximum productivity and minimum specific eluent consumption are always obtained when the maximum p_1^{CA} is chosen, *i.e.* when $p_1^{CA} = 100\%$. This stems from the fact that the local purity of the first component in the mixed wave is always lower than that in the feed. Therefore, it is more beneficial to collect the column fraction CA at 100% purity and blend it with fresh feed outside the column instead of collecting part of the mixed wave to the product fraction A. The corresponding optimal bypass ratio is $\beta^A = 1 - Y_2$, where Y_2 can be calculated from the purity constraints as shown in Eq. (7). The cut time is in that case equal to the retention time of the second shock.

5.2.2. Optimization of p_2^{CB}

Now that the optimal purity of the first column fraction is known to be $p_1^{CA} = 100\%$, the second task is to optimize p_2^{CB}. For this purpose, the dependency of V_{inj}, Δt_{cycle} and V^{PF} on p_2^{CB} is first discussed. This allows analyzing its influence on the productivity and eluent consumption.

When p_2^{CB} increases, the cut time τ_{cut} moves towards the end of the chromatogram and the mass in the column fraction CB decreases. At the same time, the injection width decreases since it is directly proportional to m_2^{CB} (column fraction CA contains no component 2 when $p_1^{CA} = 100\%$)

$$\left.\frac{\partial \Delta t_{inj}}{\partial p_2^{CB}}\right|_{p_1^{CA}=100\%} < 0 \tag{27}$$

Therefore, also the cycle time decreases with increasing p_2^{CB}, as seen by applying the chain rule to Eqs. (23) and (27)

$$\left.\frac{\partial \Delta t_{cycle}}{\partial p_2^{CB}}\right|_{p_1^{CA}=100\%} < 0 \tag{28}$$

The derivative of V^{PF} with respect to p_2^{CB} depends on the location of the cut point. For relatively high p_2^{CB} values ($p_2^{CB} > p_{2,limitA}^{CB}$) the cut point lies on the mixed wave and V^{PF} decreases when p_2^{CB} increases as seen by differentiating Eq. (2.8)

$$\left.\frac{\partial V^{PF}}{\partial p_2^{CB}}\right|_{p_1^{CA}=100\%} < 0 \tag{29}$$

In contrast, for low p_2^{CB} values ($p_2^{CB} \leq p_{2,limitA}^{CB}$), the cut point is located on the injection plateau and V^{PF} is independent of p_2^{CB}. This is observed by eliminating β^B from Eqs. (10b) and (11b) which yields

$$V^{PF} = \frac{\int_{\tau_p}^{\tau_{E2}} c_2 d\tau - ((1-p_1^{F})/p_1^{F}) \int_{\tau_p}^{\tau_{E2}} c_1 d\tau}{(Y_1+Y_2-1)c_2^{F}} Q \tag{30}$$

Table 3
Equations for solving p_2^{CB} that lead to maximum productivity in bypass operation for Langmuir isotherm. The derivative $\partial PR/\partial p_2^{CB}$ is not defined when $p_2^{CB} = p_{2,limitA}^{CB}$ or $p_2^{CB} = p_{2,limitB}^{CB}$. There are no zero points of the derivative $\partial PR/\partial p_2^{CB}$ when $p_2^{CB} < p_{2,limitA}^{CB}$. V_{col} is column volume. μ and χ are auxiliary parameters. $L_{f,i}$ is loading factor of component i.

Maximum injection volume for which the first plateau is eroded completely and corresponding p_2^{CB}

$$V_{inj} = \frac{(1-\varepsilon)(H_2-\omega_1^F)(H_1-\omega_1^F)\omega_1^F\omega_2^F}{H_1H_2(\omega_2^F-\omega_1^F)}V_{col} \tag{3.1}$$

$$p_{2,limitB}^{CB} = \left\{1 + \frac{H_2K_2(\omega_2^F-H_1)(\omega_2^F-\omega_1^F)\left[H_1-H_2+(H_2-\omega_1^F)\sqrt{(H_1-\omega_1^F)/(\omega_2^F-\omega_1^F)}\right]^2}{H_1K_1(H_1-\omega_1^F)(H_2-\omega_2^F)(H_2-\omega_1^F)^2}\right\}^{-1} \tag{3.2}$$

The zero point of the derivative $\partial PR/\partial p_2^{CB}$ *when the first plateau is not eroded and the cut point is located on the mixed wave,* $p_{2,limitA}^{CB} < p_2^{CB} < p_{2,limitB}^{CB}$

$$\mu = \frac{H_2+H_1}{2} + \frac{H_1H_2(H_2-\omega_1^F)}{2\omega_1^F\omega_2^F} \tag{3.3}$$

$$\chi = H_1H_2\left(\frac{H_2-\omega_1^F}{\omega_2^F}+1\right) \tag{3.4}$$

$$V_{inj} = \frac{(1-\varepsilon)(H_2-\omega_2^F)}{K_2H_2c_2^F(H_2-H_1)}\left(H_2-\mu+\sqrt{\mu^2-\chi}\right)^2 V_{col} \tag{3.5}$$

$$p_2^{CB} = \left[1+\frac{(1-\varepsilon)(\omega_2^F-H_1)}{K_1H_1c_2^F(H_2-H_1)}\frac{V_{col}}{V_{inj}}\left(H_1-\mu+\sqrt{\mu^2-\chi}\right)^2\right]^{-1} \tag{3.6}$$

The zero point of the derivative $\partial PR/\partial p_2^{CB}$ *when the first plateau is eroded,* $p_2^{CB} > p_{2,limitB}^{CB}$

$$V_{inj} = (1-\varepsilon)\left[\frac{K_1H_1c_1^F}{(H_1-\omega_1^S)^2}+\frac{K_2H_2c_2^F}{(H_2-\omega_1^S)^2}\right]^{-1}V_{col} \tag{3.7}$$

$$L_{f,i} = \frac{K_ic_i^FV_{inj}}{(1-\varepsilon)H_iV_{col}} \tag{3.8}$$

$$m_1^{CA} = c_1^FV_{inj} - \frac{(1-\varepsilon)(\omega_2^F-H_1)}{H_1K_1(H_2-H_1)}\left(H_1-H_2+\sqrt{\frac{H_1H_2(H_2-\omega_1^F)}{\omega_1^F\omega_2^F(1-\varepsilon)}\frac{V_{inj}}{V_{col}}}\right)^2 V_{col} \tag{3.9}$$

$$\frac{\partial m_1^{CA}}{\partial V_{inj}} = c_1^F - \frac{H_2(H_2-\omega_1^F)(\omega_2^F-H_1)}{K_1\omega_1^F\omega_2^F(H_2-H_1)} + \frac{\phi(\omega_2^F-H_1)}{H_1K_1}\sqrt{\frac{\varepsilon H_1H_2(H_2-\omega_1^F)}{\phi\omega_1^F\omega_2^F}\frac{V_{col}}{V_{inj}}} \tag{3.10}$$

$$\Delta t_{cycle} = \phi H_1\left[\alpha-\left(\frac{\omega_1^S}{H_1}\right)^2+L_{f,2}\frac{\alpha-1}{\alpha}\left(\frac{\alpha\omega_1^S}{H_2-\omega_1^S}\right)^2\right]t_0 \tag{3.11}$$

$$\frac{\partial\Delta t_{cycle}}{\partial V_{inj}} = \frac{\phi H_1t_0}{V_{inj}}\left[\frac{(\omega_1^S/H_1)^4 - L_{f,2}((\alpha-1)/\alpha)(\omega_1^S/H_1)(\alpha\omega_1^S/(H_2-\omega_1^S))^3}{L_{f,1}(\omega_1^S/(H_1-\omega_1^S))^3+(L_{f,2}/\alpha)(\alpha\omega_1^S/(H_2-\omega_1^S))^3} + L_{f,2}\frac{\alpha-1}{\alpha}\left(\frac{\alpha\omega_1^S}{H_2-\omega_1^S}\right)^2\right] \tag{3.12}$$

$$\frac{\partial m_1^{CA}}{\partial V_{inj}}\Delta t_{cycle} - \frac{\partial\Delta t_{cycle}}{\partial V_{inj}}m_1^{CA} = 0 \tag{3.13}$$

$$p_2^{CB} = \frac{c_2^F}{c_1^F+c_2^F-(m_1^{CA}/V_{inj})} \tag{3.14}$$

According to Eq. (29), the highest amount of fresh feed is processed when the purity constraint of fraction CB is as low as possible. For successful bypass operation, the lower limit is $p_2^{CB} = p_2^B$.

As seen from Eqs. (29) and (28), both V^{PF} and Δt_{cycle} (*i.e.* the numerator and the denominator of the definition of the productivity, Eq. (18)) decrease or remain constant when p_2^{CB} increase. For this reason, to find p_2^{CB} that leads to maximum productivity one must calculate *PR* at the zero points of the derivative $\partial PR/\partial p_2^{CB}$, at the points where $\partial PR/\partial p_2^{CB}$ is not defined, and at the boundaries of the interval $p_2^B - 100\%$. The correct p_2^{CB} is the one giving the largest *PR*. Analytical equations for the zero points of the derivative are given in Table 3. The calculations must be done in two steps because t_{R1} (and thus Δt_{cycle}) is evaluated from different expressions depending on whether the first component plateau is eroded or not. In the case of large injections, the first plateau prevails and an explicit expression for the zero point of the derivative is given by Eq. (3.6). For small injections, the first plateau erodes completely and Eq. (3.13) remains implicit with respect to the characteristic parameter ω_1^S that corresponds to the height of the first shock.

It is worth noting that maximum productivity is never obtained when t_{cut} is located on the injection plateau. This is because on this region V^{PF} is independent of p_2^{CB} while Δt_{cycle} increases with increasing Δt_{inj} and decreasing p_2^{CB}. Maximum *PR* is thus always obtained when $p_2^{CB} \geq p_{2,limitA}^{CB}$.

It is also interesting to note that the roots of the derivative $\partial PR/\partial p_2^{CB}$ are independent of p_1^A and p_2^B. As will be seen later in Section 7.1, maximum *PR* is achieved at the zero point of the derivative as far as corresponding p_2^{CB} is larger than p_2^B. In contrast, when p_2^{CB} at the zero point of the derivative is smaller than p_2^B, it is not possible to operate bypass with that p_2^{CB} value, and maximum *PR* is obtained at the boundary of the operation region, *i.e.* $p_2^{CB} = p_2^B$.

To evaluate the effect of p_2^{CB} on the eluent consumption, the numerator of Eq. (19) is differentiated. Again, for large injections (low p_2^{CB}) the first plateau prevails, $\partial t_{R1}/\partial\Delta t_{inj} = 0$ and V_{eluent} is constant. In the case of small injections (high p_2^{CB}), $\partial t_{R1}/\partial\Delta t_{inj} < 0$ and V_{eluent} decreases with increasing p_2^{CB}

$$\left.\frac{\partial V_{eluent}}{\partial p_2^{CB}}\right|_{p_1^{CA}=100\%} = Q\left(\frac{\partial\Delta t_{cycle}}{\partial\Delta t_{inj}}-1\right)\left.\frac{\partial\Delta t_{inj}}{\partial p_2^{CB}}\right|_{p_1^{CA}=100\%} \leq 0 \tag{31}$$

Since both V_{eluent} and V^{PF} decrease or remain constant when p_2^{CB} increases, p_2^{CB} corresponding to minimum *EC* must be calculated by using a similar approach than was applied for the maximum

productivity. As will be seen later in Section 7, the maximum productivity and minimum specific eluent consumption are not always obtained with same value of p_2^{CB}.

5.3. Validation of the optimization procedure

To validate the optimization procedure, the results of optimization equations were compared with detailed simulations. The comparison was performed by applying both linear and Langmuir isotherm models, low and high purity constraints (0.6–0.99), as well as small and large separation factors (1.1–3.0) such that all cases mentioned in Sections 5.1 and 5.2 were covered.

In the simulation study, p_1^{CA} and p_2^{CB} that lead to maximum *PR* and minimum *EC* were searched by varying V_{inj} and t_{cut} such that $p_1^{CA} \geq p_1^{A}$ and $p_2^{CB} \geq p_2^{B}$. For each combination of V_{inj} and t_{cut} values, the chromatogram was first simulated by using the analytical solution of the ideal model [13,17]. The purities of the column fractions, p_1^{CA} and p_2^{CB}, the bypass ratios, β^A and β^B, and further the performance parameters, *PR* and *EC*, were then calculated by integrating the chromatogram numerically.

The results of the optimization equations and the simulation study showed a fully agreement. In all cases, the optimal values of p_1^{CA} and p_2^{CB} were equal with accuracy of four decimals.

6. Potential extensions of the method

The above discussion was limited to systems that can be described with Langmuir or linear isotherm models. However, most of the conclusions made in Sections 4 and 5 can be extended also to other isotherm systems. As already mentioned above, the bypass ratios (Eqs. (12) and (13)) depend only on p_1^{CA} and p_2^{CB} and are independent of the isotherm type. Moreover, the design method derived in Section 4.2 is generally valid for favorable, *i.e.* convex-upward, isotherms under ideal conditions as far as the rear part of the chromatogram is independent of injection width. Unfortunately, there is no analytic solution of the ideal model available for other favorable isotherms. For this reason, it is not possible to derive analytic design equations either.

By applying similar approach as in the case of Langmuir isotherm, it is possible to show that optimal p_1^{CA} is always 100% also for other favorable isotherm systems. The only requirement is that the cycle time increases with increasing injection width and that the initial slope of the isotherm is finite. The latter constraint excludes for example the Freundlich isotherm because the duration of the chromatographic cycle is infinite and 100% purity cannot be achieved because chromatograms from consecutive injections are always overlapping.

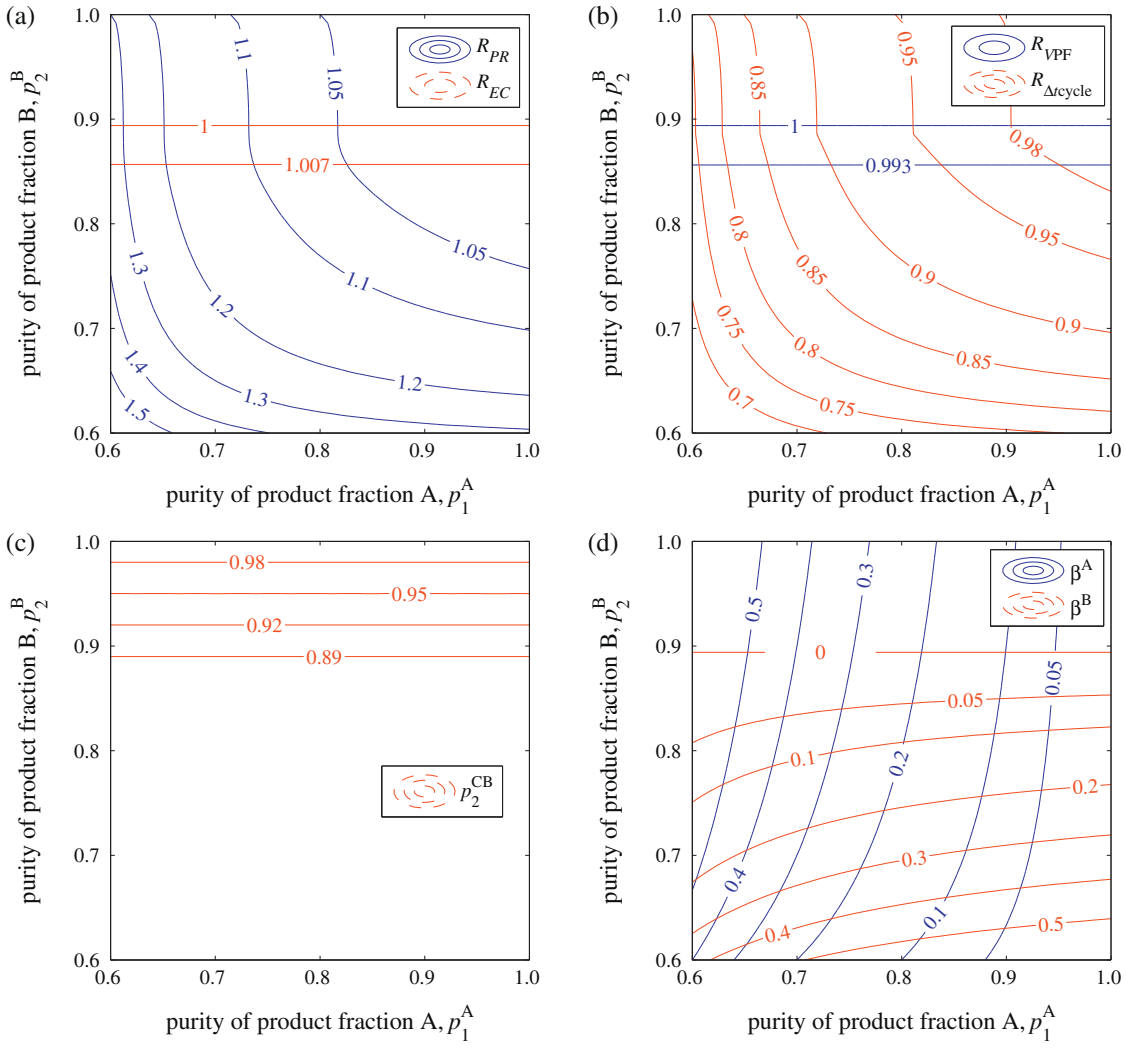

Fig. 4. Effect of purity constraints on the performance of bypass process relative to that of conventional batch chromatography when p_1^{CA} and p_2^{CB} are optimized to maximize productivity. p_1^{CA} is not shown because it is equal to 1 for the entire region. Feed concentrations: $c_1^F = c_2^F = 6$ g/L.

For unfavorable isotherm systems (*i.e.* convex-downward), such as the anti-Langmuir isotherm, an analogous but opposite approach can be used. In such cases the front of the isotherm is independent of the injection width. The cut time is obtained by searching the point where the purity constraint of the column fraction CA is satisfied. Finally, the injection width is solved from the global mass balance of the first component.

7. Demonstration of process performance under ideal conditions

The design method presented above was applied to compare the performances of the bypass and conventional operation strategies. In particular, the effects of purity constraints, feed composition, total feed concentration, and the separation factor on the productivity and the specific eluent consumption are considered.

In the performance evaluation, the separation of Tröger's base enantiomers was used as a model case. As reported by Amanullah and Mazzotti [5], the adsorption equilibrium of these enantiomers in ethanol on microcrystalline cellulose triacetate can be characterized by competitive Langmuir isotherm model. The isotherm parameters for the less absorbed enantiomer, (−)-TB, are $K_1 = 0.065$ and $H_1 = 2.18$ and for the more adsorbed enantiomer, (+)-TB, $K_2 = 0.39$ and $H_2 = 6.45$ [5,18]. The overall void fraction of the column is 0.59 [5].

7.1. Effect of purity constraints on the process performance

Since the bypass strategy can be applied only under reduced purity constraints, it is interesting to investigate the effects of p_1^A and p_2^B on the performance of bypass operation. This was done by using two optimization scenarios. Fig. 4 contains a comparison of bypass and conventional strategies when p_1^{CA} and p_2^{CB} in bypass process are optimized to maximize productivity. In Fig. 5, a corresponding comparison is provided when the bypass strategy is primarily optimized to minimize specific eluent consumption and then, if same eluent consumption is obtained with different p_1^{CA} and p_2^{CB} values, to maximize productivity.

It is observed in Fig. 4a that the productivity of bypass process is always higher than that of conventional batch chromatography. In addition, the benefit of bypass is the higher the lower the purity constraints are. This is reasonable, because for low purity constraints only a small portion of fresh feed needs to be purified in the column while the bypass fractions are relatively large (Fig. 4d). The increase in productivity achieved by using bypass results always from the decrease in the cycle time and never from the increase

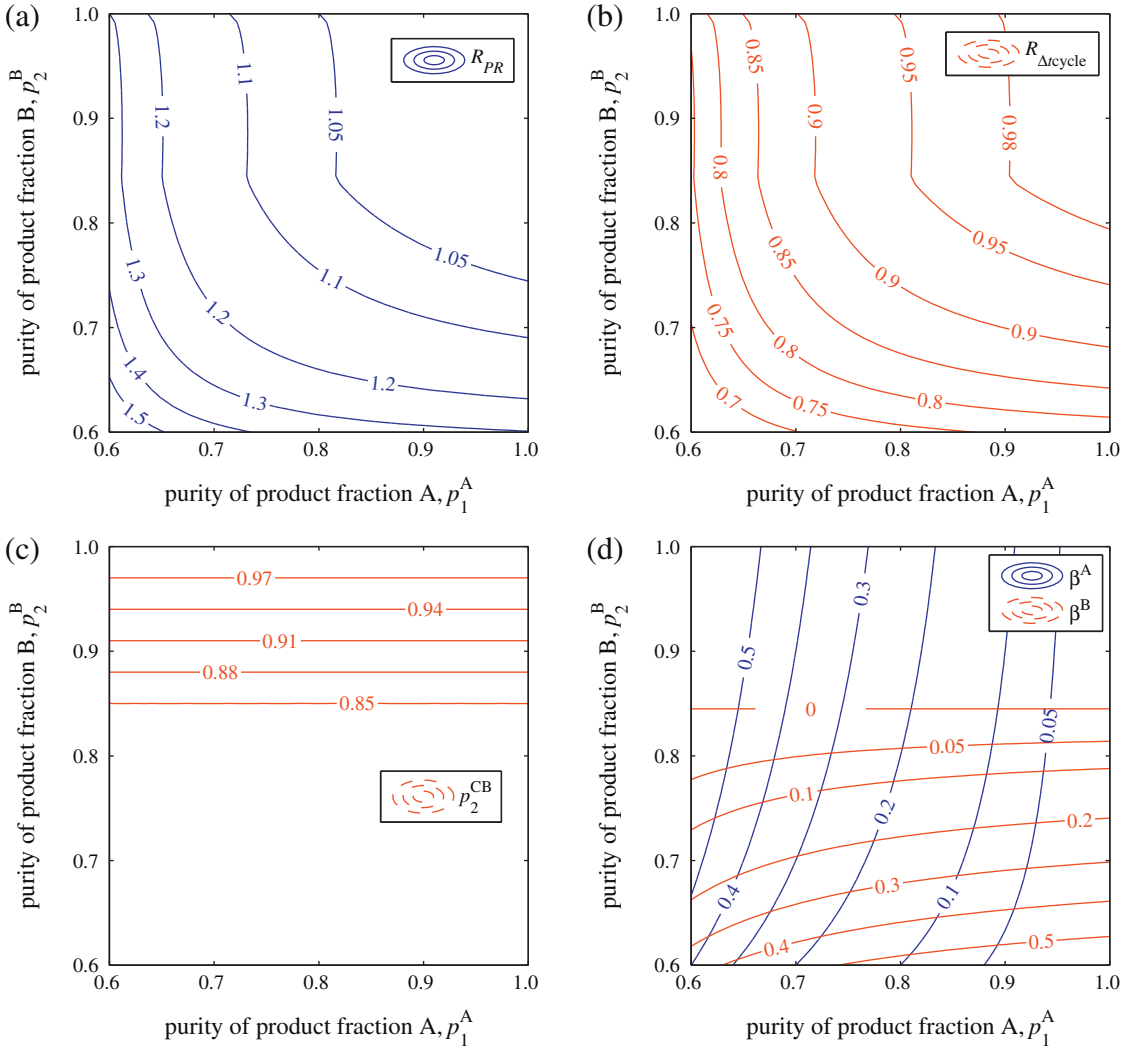

Fig. 5. Effect of purity constraints on the performance of bypass process relative to that of conventional batch chromatography when p_1^{CA} and p_2^{CB} are optimized to minimize specific eluent consumption. R_{EC}, R_{VPF}, and p_1^{CA} are not shown because they are equal to 1 for the entire region. Feed concentrations: $c_1^F = c_2^F = 6$ g/L.

in the total amount of fresh feed that can be processed per cycle (Fig. 4b).

The increase in *PR*, obtained when p_1^{CA} and p_2^{CB} are optimized with respect to productivity, is associated with only a small, if any, increase in *EC* (Fig. 4a). For example, when $p_1^A = p_2^B = 0.8$, the productivity of the bypass process is 8.4% but the specific eluent consumption only 0.7% higher than those of conventional batch process. This behavior originates from two causes. Firstly, the operating parameters for which the maximum *PR* and the minimum *EC* in the bypass process are obtained differ only slightly from each other (in fact, in both cases p_1^{CA} is always 100%). Secondly, the effects of p_1^{CA} and p_2^{CB} on *EC* are relatively small.

When p_1^{CA} and p_2^{CB} are optimized with respect to the specific eluent consumption, the *EC* of bypass strategy is equal to that of conventional batch process. However, this result is not universally valid. As will be shown later, in the cases of difficult separations where the injection volumes are small, bypass operation outperforms conventional batch chromatography also in terms of eluent consumption. In addition, it is observed in Fig. 5a that, when the bypass is optimized with respect to *EC*, it still achieves significantly higher productivity than the conventional batch process.

To obtain maximum productivity and minimum eluent consumption, the column fraction CA must always be collected at 100% purity, as was shown in Section 5.2.1. This stems from the competitive nature of the phase equilibrium. Due to the displacement effect, it is relatively easy to purify a large amount of first component to 100% purity. Moreover, the local purity of the first component in the mixed wave is always lower than that in the feed. For these reasons, it is optimal to collect the column fraction CA at 100% purity and to employ bypass strategy instead of collecting part of the mixed wave to the product fraction A.

It is observed in Figs. 4c and 5c that the optimal p_2^{CB} is independent of the purity constraint p_1^A. Depending on the value of p_2^B there exist two regions. For high p_2^B values, *i.e.* over 89% when p_1^{CA} and p_2^{CB} are optimized with respect to *PR* (Fig. 4c) and over 85% when p_1^{CA} and p_2^{CB} are optimized with respect to *EC* (Fig. 5c), it is advantageous to collect the second component from the column such that $p_2^{CB} = p_2^B$ and $\beta^B = 0$ (boundary of the operation region, see Section 5.2.2). In contrast, when p_2^B is sufficiently low, highest performance is achieved when some fresh feed is blended into the product fraction B as well (zero point of the derivative, see Section 5.2.2). In the latter case, the optimal p_2^{CB} is independent of both p_1^A and p_2^B.

7.2. Effect of feed composition on the process performance

Fig. 6 shows the influence of the feed composition on the performance of bypass operation when it is optimized with respect to productivity. The ratio of feed concentrations, c_1^F/c_2^F, is varied

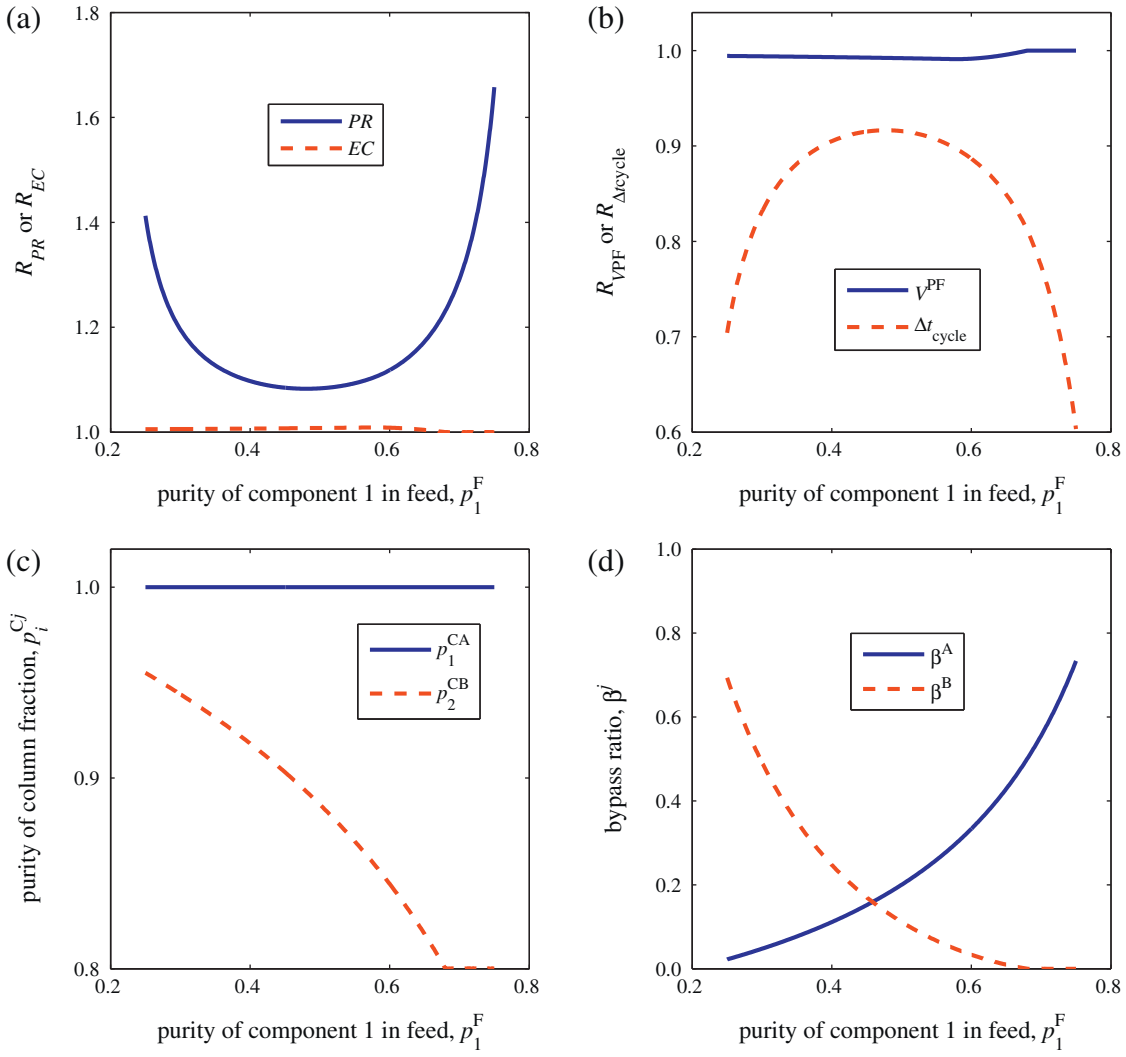

Fig. 6. Effect of feed composition on the performance of bypass process relative to that of conventional batch chromatography when p_1^{CA} and p_2^{CB} are optimized to maximize productivity. Purity constraints: $p_1^A = p_2^B = 0.8$. Total feed concentration: $c_{tot}^F = 12$ g/L.

from 1:3 to 3:1, while the total feed concentration is kept constant at 12 g/L. The purity constraints of both product fractions are set equal to 0.8.

As seen in Fig. 6a, the productivity of the bypass process compared with that of conventional chromatography is the higher the more the feed composition differs from 1:1. In fact, the productivity of bypass process tends towards infinity when p_1^F increases towards p_1^A or when p_2^F increases towards p_2^B. This is understood by considering that both for conventional and bypass processes V^{PF} increases rapidly when the feed composition approaches one or the other of the purity constraints. In the case of conventional chromatography, however, also the cycle time increases significantly because all the feed is injected into the column. In contrast, when the bypass strategy is applied, most of the feed bypasses the column and thus V_{inj} and Δt_{cycle} are almost independent of the feed composition.

The operating parameters for which maximum productivity is obtained are shown in Fig. 6c and d. The purity p_1^{CA} is again always 100% and the bypass ratio β^A is $1 - Y_2$. In contrast, optimal p_2^{CB} equals p_2^B when the first component is in large excess, and increases with increasing p_2^F. This is because only a small increase in the purity of the second component is needed in the case of high p_2^F values. However, it is worth noting that the second component should never be collected from the column at 100% purity, even if p_2^F is close to p_2^B.

7.3. Effect of total feed concentration on the process performance

The total feed concentration is an important operating parameter in many practical applications since it can be easily modified, for example by evaporating some of the solvent from the feed solution. The total feed concentration increases while the ratio of the individual feed concentrations c_1^F/c_2^F remains constant. At the same time, the competitive nature of the phase equilibrium increases, *i.e.* the separation is carried out under more non-linear conditions. To study the influence of c_{tot}^F on the performance of bypass operation c_{tot}^F was varied between 1 and 50 g/L. In reality, the solubility of Tröger's base enantiomers in ethanol is about 18 g/L [19] so all the values beyond that are hypothetical.

Fig. 7 shows the effect of c_{tot}^F on the performance of bypass operation when maximum productivity is desired. As seen in Fig. 7a, the productivity of bypass operation relative to that of conventional batch chromatography decreases when the total feed concentration increases. This can be explained as follows. The higher c_{tot}^F is, the smaller portion of the fresh feed can be bypassed and blended to the product fraction B (see the β^B-line in Fig. 7d) and, consequently, the smaller are the differences between the injection volumes (and cycle times) of the two process options (Fig. 7b). In fact, when the feed concentrations tend towards zero, the phase equilibrium tends towards linear conditions, and the purity of the column fraction CB

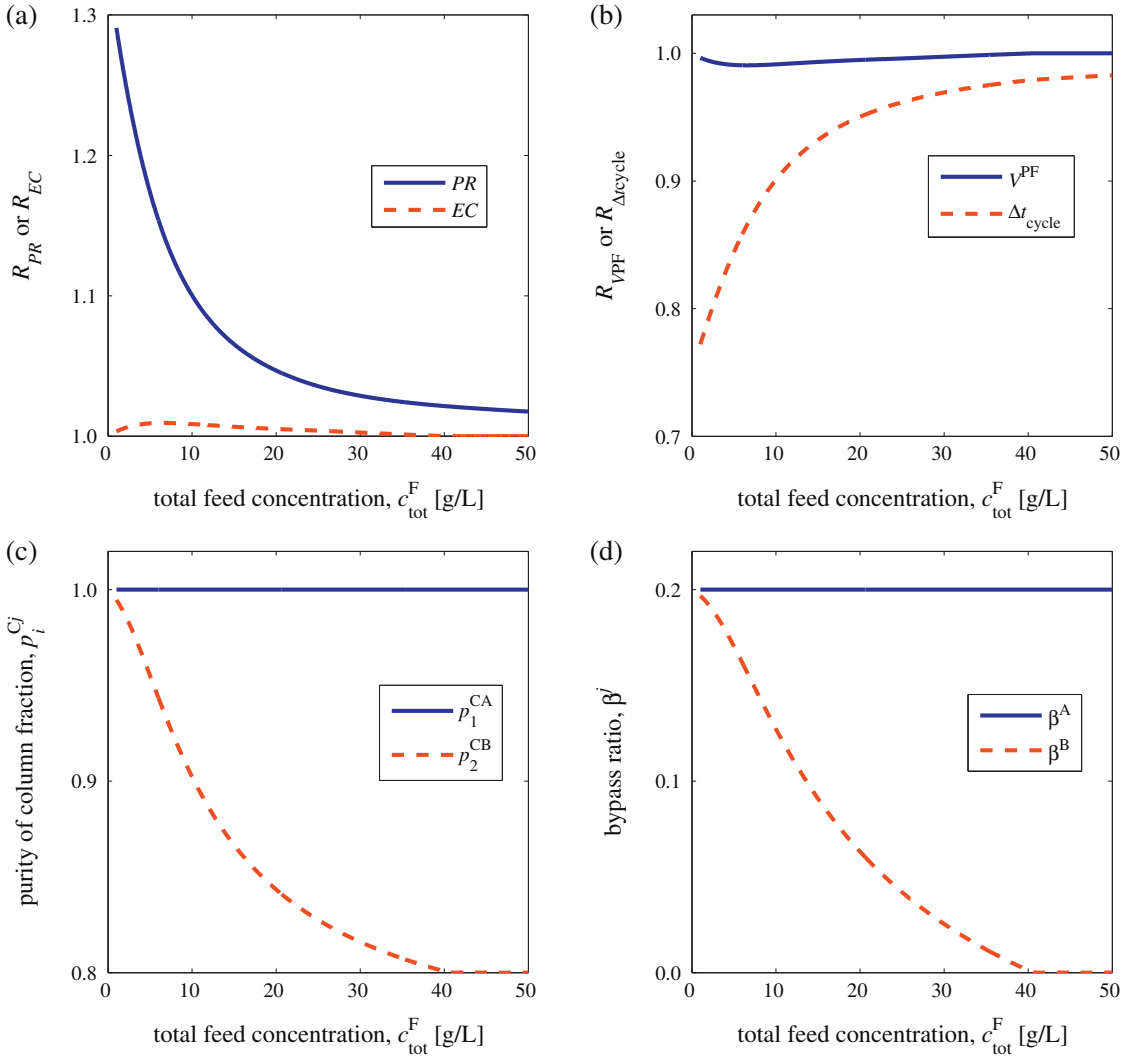

Fig. 7. Effect of total feed concentration on the performance of bypass process relative to that of conventional batch chromatography when p_1^{CA} and p_2^{CB} are optimized to maximize productivity. Purity constraints: $p_1^A = p_2^B = 0.8$. Purity of component 1 in feed: $p_1^F = 0.5$.

tends towards 100% (Fig. 7c). This is congruent with the finding for linear isotherm systems shown in Section 5.1.

As to the specific eluent consumption, it increases slightly when bypass is applied in the concentration range below 40 g/L (Fig. 7a). In contrast, for high concentrations ($c^{F}_{tot} > 40$ g/L) the maximum productivity and minimum eluent consumption of the bypass process are obtained with same operating parameters ($p_1^{CA} = 100\%$ and $p_2^{CB} = p_2^{B}$), and *EC* of the bypass strategy is equal to that of a conventional batch process.

7.4. Effect of separation factor on the process performance

The separation factor has a strong influence on process performance in preparative chromatographic separations. To investigate the effect of α on the choice of the optimal operation strategy, the Langmuir parameter of the more adsorbed enantiomer (+)-TB, K_2, was varied from 0.14 to 0.50 while K_1, $N_1 = H_1/K_1$, and $N_2 = H_2/K_2$, with N_i being the stationary phase saturation capacity of solute *i*, were kept the same as above. The simulation results are displayed in Figs. 8 and 9. Fig. 8 presents the case where p_1^{CA} and p_2^{CB} are optimized with respect to *PR* and Fig. 9 the case where they are optimized primarily with respect to *EC* and secondarily with respect to *PR*.

As to the behavior of the bypass process, there exist four regions for the separation factor. For difficult separations, $\alpha < 1.64$ in this case, *PR* of bypass process over to that of conventional process increases when the separation factor decreases (solid line in Fig. 8a). At the same time, *EC* of bypass process over that of conventional process decreases and is less than unity (dashed line in Figs. 8a and 9a). In addition, the maximum *PR* and the minimum *EC* of bypass process are obtained with the same operating parameters: $p_1^{CA} = 100\%$ and $p_2^{CB} = p_2^{B}$. This behavior is understood by considering that for difficult separations the injection volumes are so small that the first component plateau erodes completely during elution. In that case, the decrease in the injection volume obtained by using the bypass option has a strong effect on the cycle time, and thus on *PR* and *EC*, because $\partial\Delta t_{cycle}/\partial\Delta t_{inj} > 1$ (see Eq. (23)). The phenomenon becomes more pronounced when the separation factor decreases. The greatest benefit of the bypass mode is obtained when α is close to unity.

In the region $1.64 < \alpha < 1.84$, maximum *PR* and minimum *EC* of the bypass process are again obtained with $p_1^{CA} = 100\%$ and $p_2^{CB} = p_2^{B}$ (Figs. 8c and 9c). However, the separation is now easier than in the previous case. It is possible to use larger injection volumes, and the first component plateau prevails during elution also when bypass is applied. The effect of the injection width on the cycle time is now lower than with $\alpha < 1.64$ because $\partial\Delta t_{cycle}/\partial\Delta t_{inj} = 1$

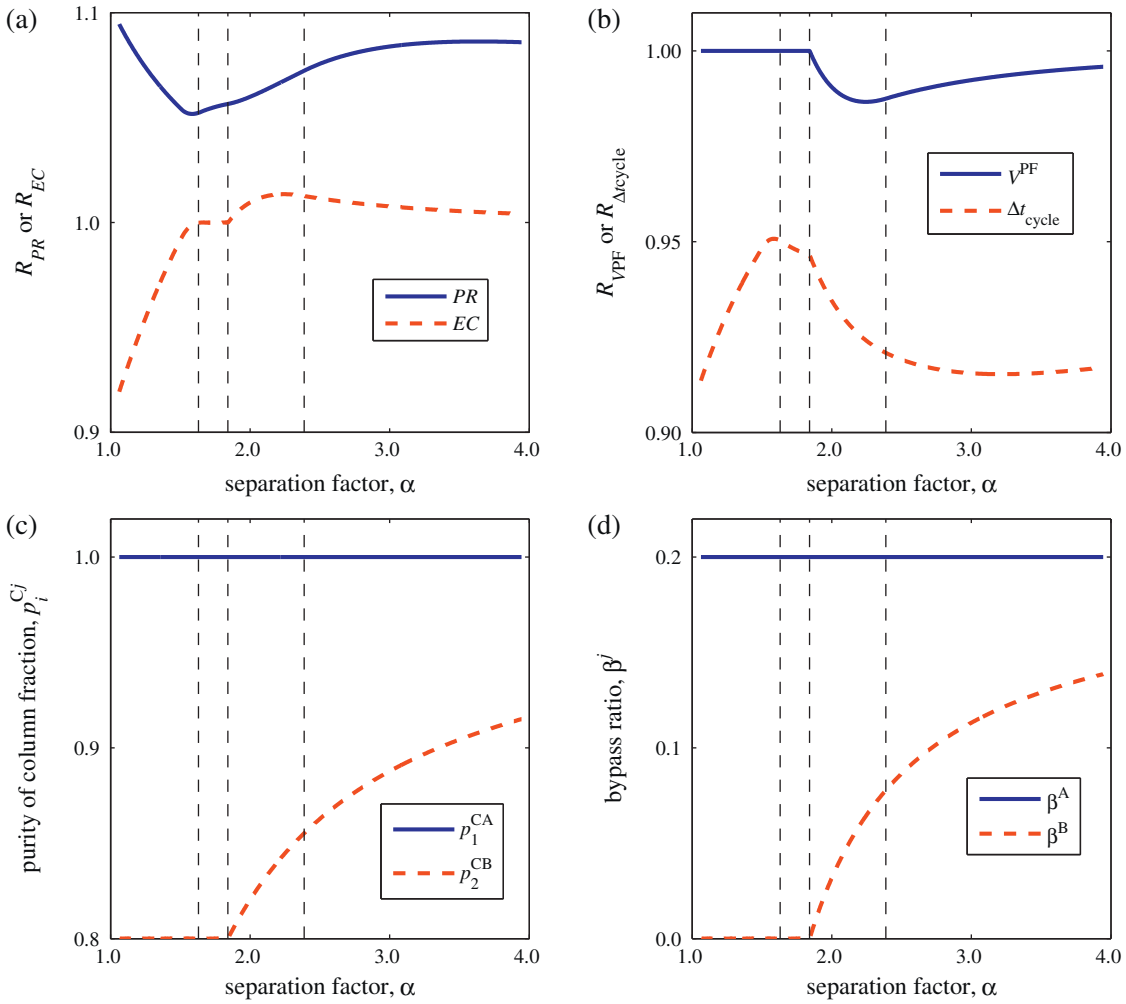

Fig. 8. Effect of separation factor on the performance of bypass process relative to that of conventional batch chromatography when p_1^{CA} and p_2^{CB} are optimized to maximize productivity. Dashed lines indicate different regions for separation factor (see text). Feed concentrations: $c_1^F = c_2^F = 6$ g/L. Purity constraints: $p_1^A = p_2^B = 0.8$. Same isotherm parameters as in the separation of Tröger's base enantiomers except K_2 is varied from 0.14 to 0.50.

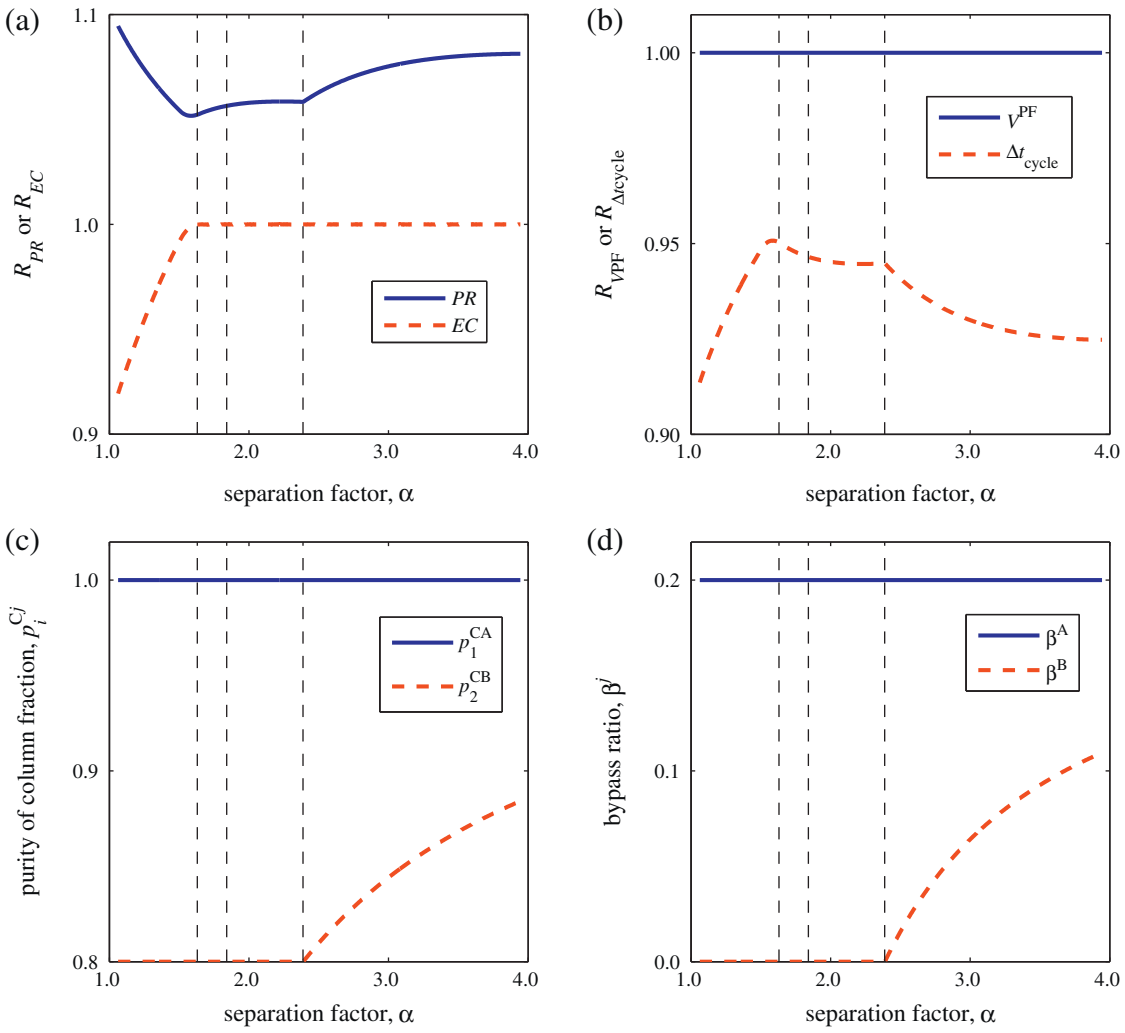

Fig. 9. Effect of separation factor on the performance of bypass process relative to that of conventional batch chromatography when p_1^{CA} and p_2^{CB} are optimized to minimize specific eluent consumption. Dashed lines indicate different regions for separation factor (see text). Feed concentrations: $c_1^F = c_2^F = 6$ g/L. Purity constraints: $p_1^A = p_2^B = 0.8$. Same isotherm parameters as in the separation of Tröger's base enantiomers except K_2 is varied from 0.14 to 0.50.

(see Eq. (23)). For this reason, *PR* of bypass strategy relative to that of conventional batch process begins to increase with increasing α while *EC* of bypass strategy is equal to that of conventional process (Figs. 8a and 9a).

When p_2^{CB} is optimized with respect to productivity (Fig. 8d) and the separation factor is increased further, the separation task becomes so easy that some bypass can be added also to the product fraction B. This increases the performance of the bypass option. As seen in Fig. 8a and d, higher bypass ratios β^B can be used with large separation factors, and the bypass process has higher productivity than the conventional mode. On the other hand, the increase in *PR* is counter-balanced by a small increase in *EC*.

In the last of the four regions, where $\alpha > 2.39$, some bypass can be added to product fraction B also when minimum *EC* is desired (Fig. 9d). In that case, the bypass option is optimized primarily with respect to *EC* and secondarily with respect to *PR*. This is because minimum *EC* is obtained when V_{inj} is so large that the injection plateau prevails and the cut point is located on it. The eluent consumption is then independent of p_2^{CB} for low p_2^{CB} values (see Eqs. (30) and (31)). To maximize the process performance, productivity must be maximized with minimum eluent consumption. This is achieved by choosing V_{inj} and the corresponding p_2^{CB} such that the injection plateau is just eroded during elution (dashed line in Fig. 9c).

8. Applicability of the design method under non-ideal conditions

To demonstrate the applicability of the equilibrium theory based approach to design real chromatographic separations (that involve dispersive effects due to mass-transfer resistances, axial dispersion, etc.) numerical simulations were carried out by using the solid film linear driving force model (for more details see, *e.g.* [1]). The separation of Tröger's base enantiomers was again used as a model case. The simulation parameters and corresponding column efficiencies are reported in Table 4.

In the numerical simulations, the cycle time was calculated as the difference between the times when the concentration of the first component at the band front and the concentration of the second component at the band tail are equal to 6×10^{-3} g/L. The operating parameters that lead to maximum productivity for given purity constraints were solved by using Matlab's optimization tools. The bypass process was optimized on two levels. At the lower level, the cut time corresponding to maximum productivity with given injection volume was searched. This algorithm was then used as a subroutine for the upper level, where the injection width was optimized by using the single-variable solver *fminbnd*. The performance of conventional batch chromatography, where both purity constraints are satisfied without waste streams, was calculated as a

Table 4
Parameter values and column efficiencies for the model systems used in numerical simulations. Numbers of theoretical stages for individual components have been calculated under linear conditions.

Parameter	Set A	Set B	Unit
Feed concentrations, c_1^F and c_2^F	6	6	g/L
Column length, L_{col}	50	50	cm
Column diameter, D_{col}	5	5	cm
Total void fraction of the bed, ε	0.59	0.59	
Particle diameter (spherical), d_p	0.02	0.05	cm
Intraparticle diffusion coefficients, $D_{p,1}$ and $D_{p,2}$	60×10^{-6}	60×10^{-6}	cm^2/min
Axial dispersion coefficients, $D_{ax,1}$ and $D_{ax,2}$	4.8×10^{-3}	4.8×10^{-3}	cm^2/min
Flow rate, Q	10	10	mL/min
Number of theoretical stages for component 1, NTP_1	870	170	
Number of theoretical stages for component 2, NTP_2	1260	260	

reference. In that case, the injection volume was searched by using the *fzero* function.

The effect of the column efficiency on the performance of bypass operation is shown in Fig. 10. The results obtained with the ideal model and the numerical simulations show similar trends. It is observed in Fig. 10a that the productivity of bypass operation relative to that of conventional batch chromatography is the higher the more efficient the column is. With this respect, the ideal model provides an upper limit for the superiority of the bypass strategy. This is obvious by considering that the more efficient the column, the easier it is to separate the components to high purities and to benefit from the bypass operation.

The component 1 must be collected from the column at higher purity than the second component also under non-ideal conditions. This stems from the displacement effect as explained in Section 7.1. As seen in Fig. 10c, p_1^A is almost independent of the final purity requirements and in fact close to 100%. In contrast, p_2^{CB} is equal to p_2^B when the purity constraints are relatively high. For low p_2^B

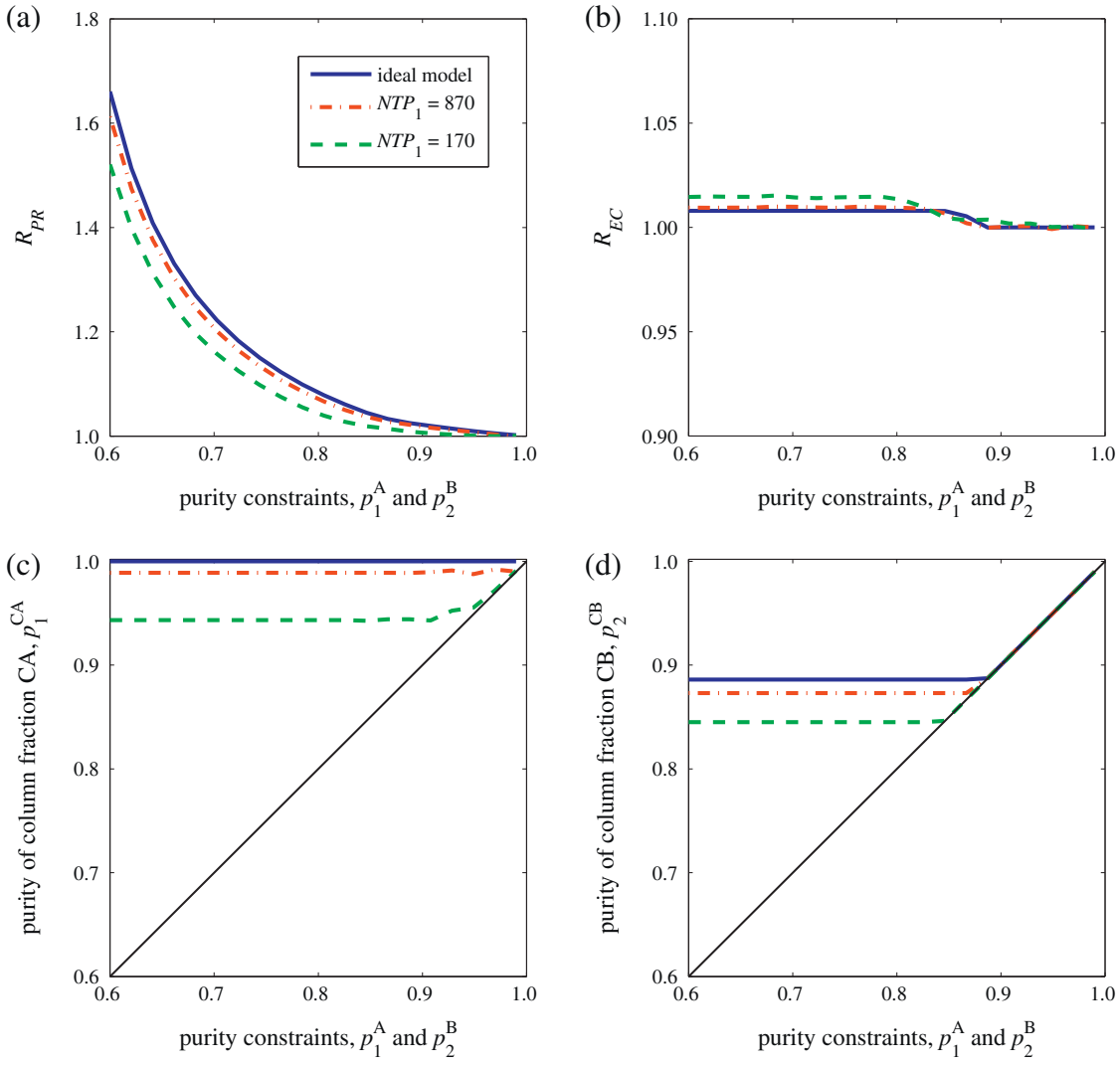

Fig. 10. Effect of column efficiency and purity constraints on the performance of bypass process relative to that of conventional batch chromatography when p_1^{CA} and p_2^{CB} are optimized to maximize productivity. Simulation parameters are given in Table 4.

values, some fresh feed can be bypassed also to the product fraction B (Fig. 10d). This is congruent with the findings based on the equilibrium theory in Section 7.1.

9. Conclusion

The possibility to apply the bypass mode of batch chromatography was investigated theoretically for the first time. A simple design method was derived by using the equilibrium theory for systems that can be described by linear or Langmuir isotherms. The approach allows direct prediction of the total amount of fresh feed that can be introduced to the process during a chromatographic cycle, the injection volume to the column, the sizes of the bypass fractions, as well as the relevant cut times.

The benefits of the bypass strategy are somewhat counterintuitive because the solution injected to the column has to be purified beyond the final purity, and its entropy thus decreased below that of the final product. However, it should be borne in mind that the fresh feed is split into two portions: one is purified in the column into two product fractions (and undergoes entropy decrease) and the other is "bypassed" (no entropy change). Finally, the bypassed fraction is mixed with the two column fractions (increase in entropy), but this requires no work. The excessive work to decrease the entropy below the final level is thus applied to a part of the fresh feed only.

Theoretical analysis of the bypass strategy revealed that, in the case of Langmuir isotherm and ideal conditions, the less retained component must always be collected from column at 100% purity to obtain maximum productivity and minimum eluent consumption. In contrast, the optimal purity of the second column fraction depends on the purity constraint of the more retained component, and is typically less than 100%. In the case of linear isotherms, the maximum productivity is obtained when the bypass process is operated with touching bands. The specific eluent consumption is independent of the purities of the column fractions and equals that of conventional batch chromatography.

The design methods developed here were used to compare bypass strategy with the conventional operation. It was shown that when the operating parameters are optimized to maximize productivity, bypass operation always outperforms conventional batch chromatography in terms of productivity with only a small, if any, increase in specific eluent consumption. This is due to decreased cycle time in bypass operation. When minimum eluent consumption is desired, the bypass process still achieves higher productivity while its eluent consumption is not higher than that of conventional chromatography.

A short demonstration of the design method for finite efficiency systems was given. The results obtained by ideal model and numerical simulations showed similar trends. In addition, it was shown that the ideal model provides an upper limit for the increase in productivity if the bypass mode is chosen instead of the conventional process.

The bypass operation can be implemented without any additional equipments or columns. In addition, the bypass strategy is more robust than conventional process because the product purities can be adjusted outside the column by controlling the amount of bypass. These features make the strategy attractive for practical purposes.

Acknowledgements

Financial support from Academy of Finland (grant No. 252688) is gratefully acknowledged.

Appendix A.

In this appendix, it is shown that allowing the chromatograms of consecutive injections to overlap does not affect the performance of conventional batch chromatography in the case of linear isotherms under ideal conditions. In other words, productivity and eluent consumption of the process are independent of the degree of overlapping between cycles as far as no waste streams are allowed.

When batch chromatography is operated such that the consecutive injections are allowed to overlap, the injection volume can be chosen freely within the following limits

$$V_{\mathrm{inj}}^{\mathrm{min}} = (1-\varepsilon)(H_2 - H_1)V_{\mathrm{col}} \tag{A.1}$$

$$V_{\mathrm{inj}}^{\mathrm{max}} = \frac{(1-\varepsilon)(H_2 - H_1)p_2^{\mathrm{B}}c_1^{\mathrm{F}}}{[p_2^{\mathrm{B}}c_1^{\mathrm{F}} - (1-p_2^{\mathrm{B}})c_2^{\mathrm{F}}]Y_2}V_{\mathrm{col}} \tag{A.2}$$

The lower limit, $V_{\mathrm{inj}}^{\mathrm{min}}$, is equal to the injection volume when conventional batch mode is operated as "touching bands". In other words, complete separation is obtained for each injection but overlapping profiles of consecutive injections decreases the product purities to the desired level. The upper limit, $V_{\mathrm{inj}}^{\mathrm{max}}$, corresponds to operation without overlapping profiles of consecutive injections.

In the case of overlapping injections, the chromatograms show a repeating pattern that consists of the following four zones: a pure first component zone, a mixed zone after the pure first component zone (caused by incomplete resolution of the injection pulse), a pure second component zone, and a mixed zone after the pure second component zone (caused by overlapping between consecutive injections). The volume of the pure first component fraction, V^{pure1}, is given by

$$V^{\mathrm{pure1}} = (t_{\mathrm{R2}}^{\mathrm{n+1}} - t_{\mathrm{E2}}^{\mathrm{n}})Q = [n\Delta t_{\mathrm{cycle}} + t_0(1+\phi H_2) - (n-1)\Delta t_{\mathrm{cycle}} - t_0(1+\phi H_2) - \Delta t_{\mathrm{inj}}]Q = (\Delta t_{\mathrm{cycle}} - \Delta t_{\mathrm{inj}})Q \tag{A.3}$$

and the volume of the pure second component fraction, V^{pure2}, by

$$V^{\mathrm{pure2}} = (t_{\mathrm{R1}}^{\mathrm{n+1}} - t_{\mathrm{E1}}^{\mathrm{n}})Q = [n\Delta t_{\mathrm{cycle}} + t_0(1+\phi H_1) - (n-1)\Delta t_{\mathrm{cycle}} - t_0(1+\phi H_1) - \Delta t_{\mathrm{inj}}]Q = (\Delta t_{\mathrm{cycle}} - \Delta t_{\mathrm{inj}})Q \tag{A.4}$$

where $t_{\mathrm{R}i}^{n+1}$ is the beginning of the elution profile of component i at $(n+1)$th cycle, $t_{\mathrm{E}i}^{n}$ is the end of the elution profile of component i at nth cycle, and n is cycle index. The rest of the chromatogram consists of mixed zones whose total volume is

$$V^{\mathrm{mix}} = V^{\mathrm{mixA}} + V^{\mathrm{mixB}} = \Delta t_{\mathrm{cycle}}Q - V^{\mathrm{pure1}} - V^{\mathrm{pure2}} \tag{A.5}$$

where V^{mixA} and V^{mixB} are the volumes of mixed fractions that are collected to product fractions A and B, respectively. The equations for product purities, Eqs. (4) and (5), can now be written in form

$$p_1^{\mathrm{A}} = \frac{c_1^{\mathrm{F}}(V^{\mathrm{pure1}} + V^{\mathrm{mixA}})}{c_1^{\mathrm{F}}(V^{\mathrm{pure1}} + V^{\mathrm{mixA}}) + c_2^{\mathrm{F}}V^{\mathrm{mixA}}} \tag{A.6}$$

$$p_2^{\mathrm{B}} = \frac{c_2^{\mathrm{F}}(V^{\mathrm{pure2}} + V^{\mathrm{mixB}})}{c_1^{\mathrm{F}}V^{\mathrm{mixB}} + c_2^{\mathrm{F}}(V^{\mathrm{pure2}} + V^{\mathrm{mixB}})} \tag{A.7}$$

To obtain the relationship between the injection volume and the cycle time, V^{pure1}, V^{pure2}, V^{mixA}, and V^{mixB} are eliminated from Eqs. (A.3)–(A.7)

$$V_{\mathrm{inj}} = Q\Delta t_{\mathrm{inj}} = \frac{p_1^{\mathrm{F}}(1-p_1^{\mathrm{F}})(p_1^{\mathrm{A}} + p_2^{\mathrm{B}} - 1)}{p_1^{\mathrm{A}}[p_2^{\mathrm{B}} - (1-p_1^{\mathrm{F}})^2] - p_2^{\mathrm{B}}(p_1^{\mathrm{F}})^2}Q\Delta t_{\mathrm{cycle}} \tag{A.8}$$

By substituting Eq. (A.8) to the definitions of productivity and eluent consumption, Eqs. (18) and (19), the following expressions are obtained for *PR*

$$PR = \frac{p_1^F(1-p_1^F)(p_1^A+p_2^B-1)}{p_1^A[p_2^B-(1-p_1^F)^2]-p_2^B(p_1^F)^2} c_{tot}^F Q \tag{A.9}$$

and for *EC*

$$EC = \frac{(p_1^A-p_1^F)(p_1^F+p_2^B-1)}{p_1^F(1-p_1^F)(p_1^A+p_2^B-1)} \frac{1}{c_{tot}^F} \tag{A.10}$$

As seen above, both the productivity and the eluent consumption are independent of the injection volume and the cycle time. In other words, the performance of single column batch chromatography (conventional or bypass mode) cannot be improved by allowing the chromatograms of consecutive injections to overlap in the case of linear isotherms.

References

[1] G. Guiochon, A. Felinger, D.G. Shirazi, A.M. Katti, Fundamentals of Preparative and Nonlinear Chromatography, 2nd ed., Academic Press, Amsterdam, 2006.
[2] J.A. Kent (Ed.), Kent and Riegel's Handbook of Industrial Chemistry and Biotechnology, vol. 2, 11th ed., Springer, New York, 2007, p. 1686.
[3] A. Garrison, Environ. Sci. Technol. 40 (2006) 16.
[4] M. Kaspereit, K. Gedicke, V. Zahn, A.W. Mahoney, A. Seidel-Morgenstern, J. Chromatogr. A 1092 (2005) 43.
[5] M. Amanullah, M. Mazzotti, J. Chromatogr. A 1107 (2006) 36.
[6] A. Rajendran, J. Chromatogr. A 1185 (2008) 216.
[7] M. Kaspereit, A. Seidel-Morgenstern, A. Kienle, J. Chromatogr. A 1162 (2007) 2.
[8] T. Sainio, M. Kaspereit, Sep. Purif. Technol. 66 (2009) 9.
[9] M. Kaspereit, T. Sainio, Chem. Eng. Sci. 66 (2011) 5428.
[10] J. Siitonen, T. Sainio, M. Kaspereit, Sep. Purif. Technol. 78 (2011) 21.
[11] S. Golshan-Shirazi, G. Guiochon, Anal. Chem. 61 (1989) 1276.
[12] S. Golshan-Shirazi, G. Guiochon, Anal. Chem. 61 (1989) 1368.
[13] S. Golshan-Shirazi, G. Guiochon, J. Phys. Chem. 93 (1989) 4143.
[14] H.-K. Rhee, R. Aris, N.R. Amundson, First-order partial differential equations. Theory and Application of Single Equations, vol. I, Dover Publications, New York, 2001.
[15] H.-K. Rhee, R. Aris, N.R. Amundson, First-order partial differential equations. Theory and Application of Hyperbolic Systems of Quasilinear Equations, vol. II, Dover Publications, New York, 2001.
[16] A. Rajendran, M. Mazzotti, Ind. Eng. Chem. Res. 50 (2011) 352.
[17] J. Siitonen, T. Sainio, J. Chromatogr. A 1218 (2011) 6379.
[18] M. Pedeferri, G. Zenoni, M. Mazzotti, M. Morbidelli, Chem. Eng. Sci. 54 (1999) 3735.
[19] J. Worlitschek, M. Bosco, M. Huber, V. Gramlich, M. Mazzotti, Helv. Chim. Acta 87 (2004) 279.